

Nitroxide-Containing Amphiphilic Random Terpolymers for Marine Antifouling and Fouling-Release Coatings

Riddhiman Medhi,[△] Alicia Cintora,[△] Elisa Guazzelli, Nila Narayan, Amanda K. Leonard, Giancarlo Galli, Matteo Oliva, Carlo Petti, John A. Finlay, Anthony S. Clare, Elisa Martinelli,* and Christopher K. Ober*



Cite This: *ACS Appl. Mater. Interfaces* 2023, 15, 11150–11162



Read Online

ACCESS |

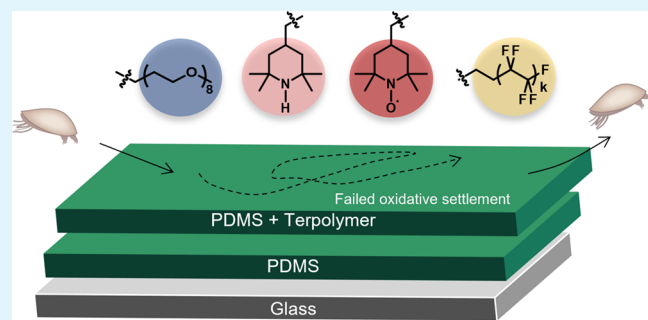
Metrics & More

Article Recommendations

Supporting Information

ABSTRACT: Two types of amphiphilic random terpolymers, poly(ethylene glycol methyl ether methacrylate)-*ran*-poly(2,2,6,6-tetramethylpiperidinyloxy methacrylate)-*ran*-poly(polydimethyl siloxane methacrylate) (PEGMEMA-*r*-PTMA-*r*-PDMSMA), were synthesized and evaluated for antifouling (AF) and fouling-release (FR) properties using diverse marine fouling organisms. In the first stage of production, the two respective precursor amine terpolymers containing (2,2,6,6-tetramethyl-4-piperidyl methacrylate) units (PEGMEMA-*r*-PTMPM-*r*-PDMSMA) were synthesized by atom transfer radical polymerization using various comonomer ratios and two initiators: alkyl halide and fluoroalkyl halide. In the second stage, these were selectively oxidized to introduce nitroxide radical functionalities. Finally, the terpolymers were incorporated into a PDMS host matrix to create coatings. AF and FR properties were examined using the alga *Ulva linza*, the barnacle *Balanus improvisus*, and the tubeworm *Ficopomatus enigmaticus*. The effects of comonomer ratios on surface properties and fouling assay results for each set of coatings are discussed in detail. There were marked differences in the effectiveness of these systems against the different fouling organisms. The terpolymers had distinct advantages over monopolymer systems across the different organisms, and the nonfluorinated PEG and nitroxide combination was identified as the most effective formulation against *B. improvisus* and *F. enigmaticus*.

KEYWORDS: fouling-release surfaces, antifouling surfaces, copolymer, polydimethylsiloxane, antioxidant, stable radical, algae, barnacle



INTRODUCTION

Marine biofouling, the unwanted process of colonization and growth of organisms on immersed surfaces, has been an issue of concern in the marine industry for many years. Bacteria can adhere to surfaces within minutes.¹ Within days and weeks, larger organisms like diatoms, algae, barnacles, and sponges will follow, although the process is not necessarily sequential and can occur within hours.^{2,3} The initial attachment of “soft foulants” such as bacteria to surfaces is reversible and primarily due to van der Waals forces. Following this, the cells will further anchor to the surface via the production of extracellular polymeric substances. “Hard foulants” such as mussels and barnacles that have a calcareous shell, on the other hand, use specialized adhesives to stick to surfaces. Mussel adhesive proteins rely on 3,4-dihydroxy-L-phenyl-alanine (L-DOPA) for their adhesion and on quinones for their cross-linking process, through radical based mechanisms.^{4–6} Barnacles instead have complicated adhesive mechanisms that are different for the cypris larvae and the adult and are still not fully understood. Studies, however, indicate that postmetamorphosis, their adhesive cross-linking relies on both

quinone and disulfide bond-based radical-driven mechanisms.^{6–9}

The adhesion of these various organisms on ships’ hulls results in significantly increased fuel use and associated costs due to the reduction of ship speed and increased maintenance, which in turn leads to increased greenhouse gas emissions.^{10,11} Various methods to combat the impact of marine biofouling have been explored. Finding a universal coating that is both nontoxic and effective at inhibiting the complex diversity in marine organism adhesion has remained a challenge. However, commercial and military vessels may operate in different maritime regions, and with their exposure to different marine organisms, it is imperative to find coatings that are broad spectrum in their activity.

Received: December 28, 2022

Accepted: February 6, 2023

Published: February 21, 2023



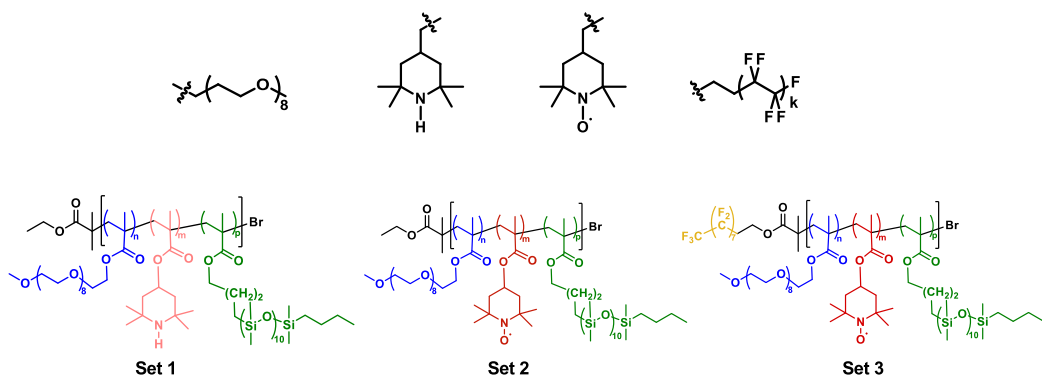


Figure 1. Chemical structures and color codes for terpolymers of Sets 1, 2, and 3 with PEG, amine, TEMPO, and fluoro end-cap functionalities.

Biocide-free polymer-based coatings are considered to be environmentally benign alternatives that provide protection against the settlement of marine organisms because they can be synthesized to contain a variety of prerequisite properties.¹² For example, hydrophobic, low surface energy polymers, such as poly(dimethylsiloxane) (PDMS) and fluoropolymers,^{1,13,14} interfere with bioadhesion and facilitate the release of fouling organisms. Additionally, PDMS provides notable mechanical properties; the low elastic modulus allows them to be readily incorporated into coatings for a variety of surfaces.¹⁵ However, highly hydrophobic materials will tend to migrate away from the water interface in aqueous environments. Hydrophilic polymers with similar surface energies to water, like poly(ethylene glycol) (PEG), surface segregate toward the water interface and can aid in anchoring PDMS or fluorinated species to the coating surface when copolymerized with more hydrophobic counterparts. PEG has also shown promise in reducing the adsorption of proteins at surfaces, a highly desirable characteristic for antifouling use.^{16–18} By combining both hydrophilic and hydrophobic polymers, amphiphilic copolymers have been produced and incorporated successfully in a number of novel coating formulations.^{19–26} Ongoing research of such systems has been reviewed.¹²

The materials prepared and presented here were inspired by the established success of amphiphilic polymers and the recent promise shown by amine²⁷ and nitroxide functionalities.²⁸ The goal is to control fouling through both surface chemistry and the inclusion of functionalities that inhibit radical chemistries. As an added functionality to polymers, nitroxides such as the 2,2,6,6-tetramethylpiperidine-1-oxyl (TEMPO) group have also provided successful antifouling properties against bacterial biofilms.^{29–31} For example, Boase et al.³² showed a reduction in bacterial biofilm growth by >99% using copolymers of (2,2,6,6-tetramethyl-1-piperidinyl)oxyl methacrylate (PTMA) with methyl methacrylate. Many hard foulers rely on radical-based cross-linked adhesives; therefore, nitroxides which can serve as antioxidant groups, have the potential to inhibit this mechanism and to limit their attachment. Previous work from the Ober group^{33,34} has utilized polymer blends of PS-*b*-PTMA and PS-*b*-P(DMS/PEG) to combine the specific properties and functionalization at the surface of antifouling coatings. Tests against the barnacle *Balanus amphitrite* showed a reduction in adhesion strength on the surface of these coatings, compared to blends without PTMA. More recent work where TEMPO and PEG were attached to a PS-PDMS backbone has shown that co-attachment of TEMPO and PEG in the same polymer promoted surface expression of TEMPO producing exceptional fouling-release performance.³³

Given the initial success of preliminary experiments incorporating TEMPO units within amphiphilic polymers, a study to test new TEMPO-based materials in a PDMS host matrix has been here initiated. Combining our experience of producing TEMPO-based polymers using controlled polymerization methods with a new amphiphilic composition and design, novel polymers were prepared to investigate their incorporation into fouling-release (FR) coatings and their effectiveness against different foulers. In this study, methacrylate random terpolymers consisting of the amphiphilic PEG/PDMS pendant functionalities and TEMPO moieties were synthesized via atom transfer radical polymerization (ATRP) (Figure 1). These materials were designed to combine the benefits that amphiphilic polymers provide, while introducing TEMPO pendant groups to the polymer backbone. In fact, homogeneous surfaces composed of multifunctional polymers with both hydrophobic and hydrophilic groups are effective at prohibiting settlement, as they do not provide marine organisms the opportunity to locate a suitable site for settlement.^{12,35}

Specifically, this article studies random terpolymers composed of PEG, TEMPO (PTMA), its amine precursor (PTMPM), and PDMSMA, in addition to a corresponding set with a fluorinated end-cap block. To access the efficiency of these random copolymers in marine antifouling applications, these polymers were coated as a blend with PDMS onto glass slides and tested against three common marine fouling organisms. The green alga, *Ulva linza*, and the barnacle, *Balanus improvisus* (= *Amphibalanus improvisus*) are frequently found on vessels operating in temperate waters. In addition, the efficiency of the TEMPO radical chemistry was evaluated against another hard fouling species, the tubeworm *Ficopomatus enigmaticus*. *F. enigmaticus*, a member of the Serpulidae family of polychaetes, is an invasive macrofouling species that naturally forms massive reefs but colonizes vessels and other hard substrates where its removal incurs considerable economic costs.^{36–38} AF and FR bioassays with these three different types of marine organism will allow us to elucidate the individual effectiveness of the various functional groups and their combinations, in random copolymer systems, to identify compositions for fouling-resistant coatings. Surface characterization of the coatings was carried out using contact angle goniometry, X-ray photoelectron spectroscopy (XPS), and atomic force microscopy (AFM), providing information on the surface chemistry and surface wettability contributions toward improving performance to combat marine fouling.

■ EXPERIMENTAL SECTION

Materials. Ethyl 2-bromoisobutyrate (EBiB), *N,N,N',N',N''*-pentamethyldiethylenetriamine (PMDETA), 2,2,6,6-tetramethyl-4-piperidyl methacrylate (TMMPM), and sodium tungstate dihydrate ($\text{Na}_2\text{WO}_4 \cdot 2\text{H}_2\text{O}$) were all purchased from Sigma-Aldrich and used as received. Sodium ethylenediamine tetraacetate dihydrate ($\text{Na}_2\text{EDTA} \cdot 2\text{H}_2\text{O}$) and hydrogen peroxide (H_2O_2) were purchased from Fischer Scientific and used as received. Copper bromide (CuBr) was purchased from Sigma-Aldrich and purified according to literature procedures.³⁹ Monomethacryloxypropyl-terminated polydimethylsiloxane ($M_n = 1000 \text{ g mol}^{-1}$, PDMSMA), purchased from Gelest, and poly(ethylene glycol) methyl ether methacrylate ($M_n = 500 \text{ g mol}^{-1}$, PEGMEMA), purchased from Sigma-Aldrich, were passed through a basic alumina column to remove the inhibitor. 17F-EBiB was synthesized as previously described in the literature.^{40–42} For coating fabrication, bisilanol-terminated PDMS ($M_n = 26,000 \text{ g mol}^{-1}$, HO-PDMS-OH) and polydiethoxysiloxane ($M_n = 134 \text{ g mol}^{-1}$, ES40) were purchased from Gelest; bismuth neodecanoate (BiND) and tetra-*n*-butylammonium fluoride (TBAF), purchased from Sigma-Aldrich, were used as received.

Synthesis of PEGMEMA-*r*-PTMPM-*r*-PDMSMA and Fluoro End-Capped PEGMEMA-*r*-PTMPM-*r*-PDMSMA. The ethyl 2-bromoisobutyrate (EBiB) initiator was used for synthesizing the PEGMEMA-*r*-PTMPM-*r*-PDMSMA polymers (Set 1), while 17F-EBiB was used as the initiator for synthesizing the fluoro end-capped PEGMEMA-*r*-PTMPM-*r*-PDMSMA terpolymers (Set F). The initiator, ligand, catalyst, and monomer ratios are listed in Table S1 and Figures S1 and S2.

We describe the polymer synthesis using example F3: 10 mL of toluene, 69.5 μL of PMDETA ($3.33 \times 10^{-4} \text{ mol}$), 0.221 g of 17F-EBiB ($3.33 \times 10^{-4} \text{ mol}$), 2.25 g of TMMPM (0.01 mol), 1.54 mL of PEGMEMA (3.33 mmol), and 3.47 mL of PDMSMA (3.33 mmol) were put in a Schlenk tube and stirred until homogenous with a magnetic stir bar. The solution was freeze–pump–thawed for 3 cycles before 47.8 mg of CuBr ($3.33 \times 10^{-4} \text{ mol}$) was added under Ar. The solution underwent three additional freeze–pump–thaw cycles and was then heated to 70 °C under stirring for 24 h. To quench polymerization, the solution was opened to air, diluted with CH_2Cl_2 , and repeatedly passed through a basic alumina column to completely remove the copper/catalyst complex. The polymer solution was then rotary-evaporated and dried under reduced pressure overnight to remove the residual solvent, yielding a yellow, viscous fluid. The polymer was then dissolved in unstabilized THF, injected into a dialysis tube (cutoff molecular weight of 7 kg mol^{-1}), and stirred at room temperature in unstabilized THF for 3 days to remove unreacted TMMPM monomers from the polymer. The resulting polymer was dried overnight under reduced pressure overnight. The polymer was then precipitated in water to remove the PEGMEMA monomer and centrifuged three times at 7000 rpm for 10 min. The remaining polymer was collected and dried under reduced pressure overnight. This synthesis yielded the polymers for Sets 1 and F, and the precursors for Sets 2 and 3 were obtained through oxidation, as described in the next section.

Oxidation to Nitroxide (PTMA). The synthesis recipe for the oxidation of PTMPM to PTMA was modified from a previously reported recipe,⁴³ as illustrated in Figure S5. In the typically modified recipe, polymers synthesized in the previous step containing PTMPM (232 mg, 1.03 mmol of amine functions, 1 equiv.), $\text{Na}_2\text{WO}_4 \cdot 2\text{H}_2\text{O}$ (170 mg, 0.52 mmol, 0.50 equiv.), $\text{Na}_2\text{EDTA} \cdot 2\text{H}_2\text{O}$ (90 mg, 0.30 mmol, 0.30 equiv.), and methanol (12 mL) were added to a three-neck round-bottom flask with a condenser. The solution was stirred at 60 °C for 5 min and H_2O_2 (2.34 mL, 20.6 mmol, 20 equiv.) was added dropwise over 60 min. The mixture was further stirred at 60 °C for 48 h. The polymer was extracted with CH_2Cl_2 , and the organic solution was washed repeatedly with water and dried with anhydrous MgSO_4 . After filtration, the solution was concentrated and precipitated in cold hexane, filtered, and dried under vacuum at 40 °C overnight. This procedure yielded polymers for Sets 2 and 3.

Coating Preparation. PDMS was deposited in two steps onto acetone-cleaned and dried glass slides ($76 \times 26 \text{ mm}^2$) following an established procedure.²⁰ In a typical preparation of film, in the first step, the matrix consisting of 5.0 g of HO-PDMS-OH, 0.125 g of cross-linker ES40, and 50 mg of catalyst BiND was dissolved in 25 mL of ethyl acetate. The solution was spray-coated using a Badger 250 airbrush. The films were dried at room temperature for one day and annealed at 120 °C for the second day. In the second step, a solution of the same composition, but also containing 200 mg of the chosen terpolymer (4 wt % concentration as a fraction of the PDMS matrix), was spray-coated on top of the first layer and cured at room temperature for 2 days and subsequently at 120 °C for 1 day (overall thickness ca. 10 μm). An analogous two-layer blank PDMS film (i.e., without terpolymer) was used as a control.

Preparation of Coatings for Biological Assays. Three-layer films were deposited on glass slides ($76 \times 26 \times 1 \text{ mm}^3$), previously washed with acetone and dried in a vacuum oven at 120 °C for 12 h. Films were prepared according to an established three-step procedure.^{44,45} The first step consisted of spray-coating a solution of the matrix HO-PDMS-OH (5 g), the cross-linker ES40 (0.125 g), and the catalyst TBAF (15 mg) dissolved in 15 mL of ethyl acetate. The films were dried at room temperature overnight. In the second step, a solution of the same composition was deposited on the bottom layer (to obtain a final dry thickness of ca. 300 μm). The films were dried at room temperature for 1 day and annealed at 120 °C for 12 h. Finally, a top layer was formed by spray coating the PDMS-based formulation reported above in which the copolymer additive (4 wt % as a fraction of PDMS) was added. After the deposition of the top layer, the films were left at room temperature for 12 h and then thermally annealed in a vacuum oven at 120 °C for 12 h. An analogous three-layer blank PDMS film (i.e., without terpolymer, coating 12) was used as a control.

Fouling Assays. *U. linza* and *B. improvisus*. Settlement and removal assays for *U. linza* and *B. improvisus* were conducted as per previously reported methods.^{20,25,33}

F. enigmaticus. Settlement assays for *F. enigmaticus* were performed according to a slight modification of an established procedure.^{44,47} Adults were collected in S. Rossore-Migliarino-Massaciuccoli Regional Park (Pisa, Italy) and acclimated in the laboratory to test conditions (temperature 20 ± 2 °C, water salinity 30 ppt, pH 8.12, 14 h light: 10 h dark photoperiod) prior to use.⁴⁴ Larval culture for the test setup was as follows: male and female gamete release was obtained by gently breaking the calcareous tubes, removing the serpulid worms and placing them singularly in the wells of 24-well plates filled with 0.45 μm filtered seawater (salinity 30 ppt). After gametes were released, sperms from different males were pooled, and the final concentration was measured with a Burker cell-counting chamber and an optical microscope. In the meanwhile, eggs of different females were pooled and rinsed 3 times with clean 0.45 μm filtered seawater, in order to remove broken and immature eggs. A fertilization suspension ($\sim 800 \text{ mL}$) was then prepared exposing the clean egg suspension to a sperm concentration of about $3–4 \times 10^4 \text{ sperms mL}^{-1}$. Fertilization usually occurred within 1 h, while first swimming larval development occurred within 18–24 h. The larval stage needed for settlement assays was the “competent larva,” i.e., a larva that has lost its swimming ability and has started to crawl on hard substrata, actively searching for settlement spots. This stage is usually reached 9–10 days after fertilization. Larvae were reared at 20 ± 2 °C, under a 14 h light:10 h dark photoperiod and fed ad libitum with a *Isochrysis galbana* suspension ($\sim 10^5 \text{ cells mL}^{-1}$) until they reached the “competent larva” stage. When the desired stage was reached, the larval suspension was filtered through a 30 μm nylon net and the collected larvae were resuspended in a small volume of fresh seawater ($\sim 50 \text{ mL}$). Simultaneously, sample slides, previously maintained in 0.45 μm filtered seawater for 48 h, were rinsed in distilled water and placed in 4-well Quadriperm plates (6 replicates per formulation). One milliliter drops of clean seawater were put on each slide; then, 20 competent larvae were pipetted in each drop. All plates were then incubated in darkness at 20 ± 2 °C and covered with wet towels to prevent evaporation. Incubation was performed for a

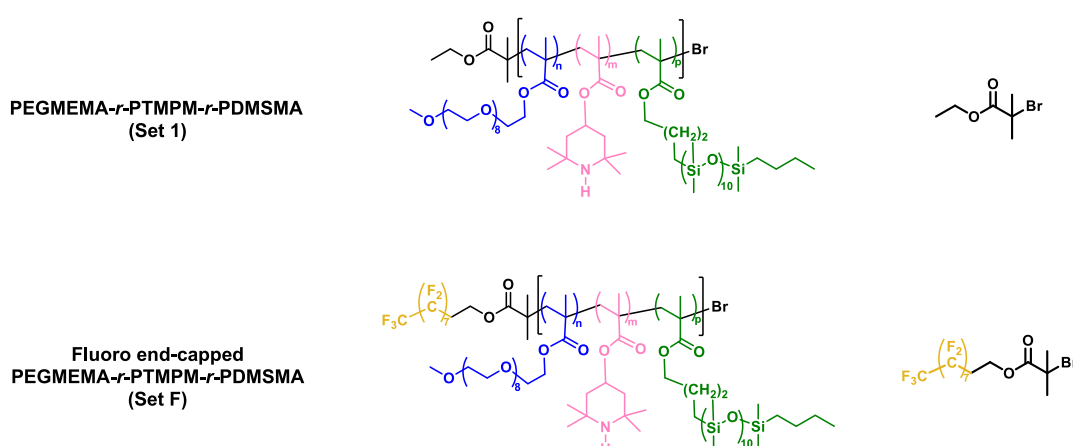


Figure 2. Scheme of PEGMEMA-*r*-PTMPM-*r*-PDMSMA terpolymers of Set 1 (top) and Set F (bottom).

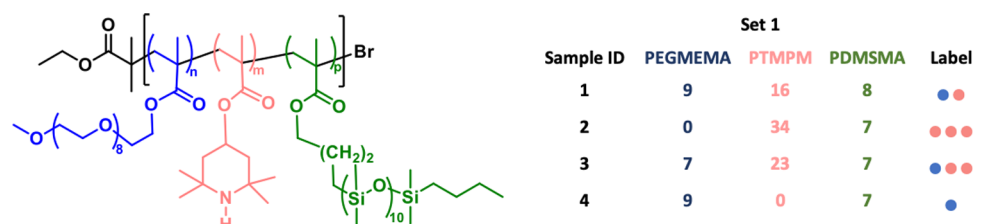


Figure 3. Chemical structure, sample ID, comonomer repeat units, and color labels for the amine terpolymers of Set 1. Colored labels are the approximate relative amounts of PEGMEMA (blue), PTMPM (pink), and PDMSMA in the polymers, shown here for ease of identification.

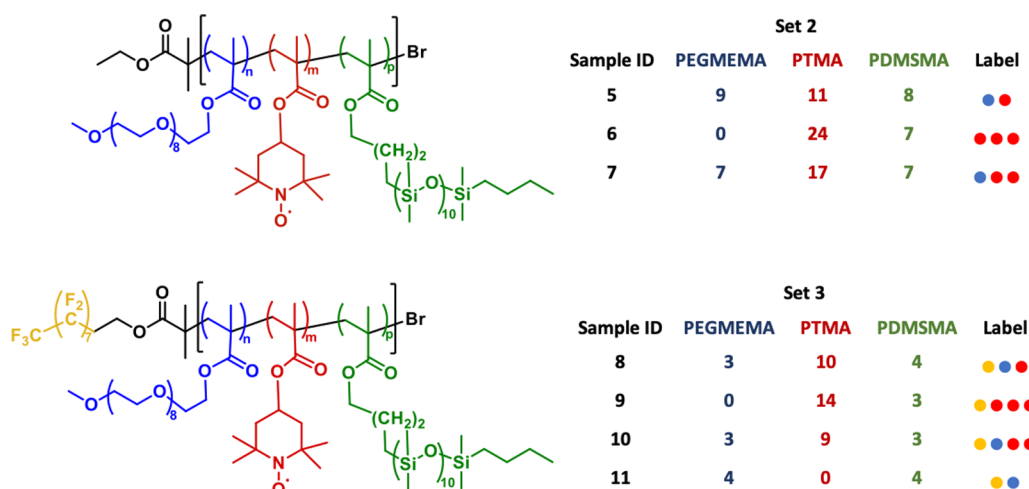


Figure 4. Chemical structures, sample ID, comonomer repeat units, and color labels for the TEMPO and fluorinated-TEMPO terpolymer Sets 2 and 3, respectively. Colored labels are the approximate relative amounts of PEGMEMA (blue), PTMA (red), PDMSMA, and fluorinated end cap (yellow) in the polymers of Sets 2 and 3, shown here for ease of identification.

total time of 5 days. Percentage settlement was then calculated. PDMS-covered slides acted as the control. PERMANOVA analysis, followed by the Monte Carlo post-test, was performed for all coatings to determine differences in the percentages of *F. enigmatus* settlement among all coating samples.

RESULTS AND DISCUSSION

Material Preparation. Synthesis of Terpolymers. Two polymer sets were synthesized consisting of random terpolymers with varying ratios of PEGMEMA, PTMPM, and PDMSMA (Figure 2). Two alkyl halide initiators were chosen:

EBiB (for Set 1) and 17F-EBiB (for Set F). EBiB is commonly used as a hydrophobic ATRP initiator and in numerous preparations of poly(methacrylate)s. 17F-EBiB was employed in our system in order to introduce an additional fluorinated functionality to the polymer end group. Studies have in fact shown that while fluorinated components are necessary to bring their comonomer counterparts to the surface, too much fluorination at the surface can be detrimental for antifouling efficacy.²¹ This is due to the high interfacial energy between fluorinated materials and water, where marine organisms are

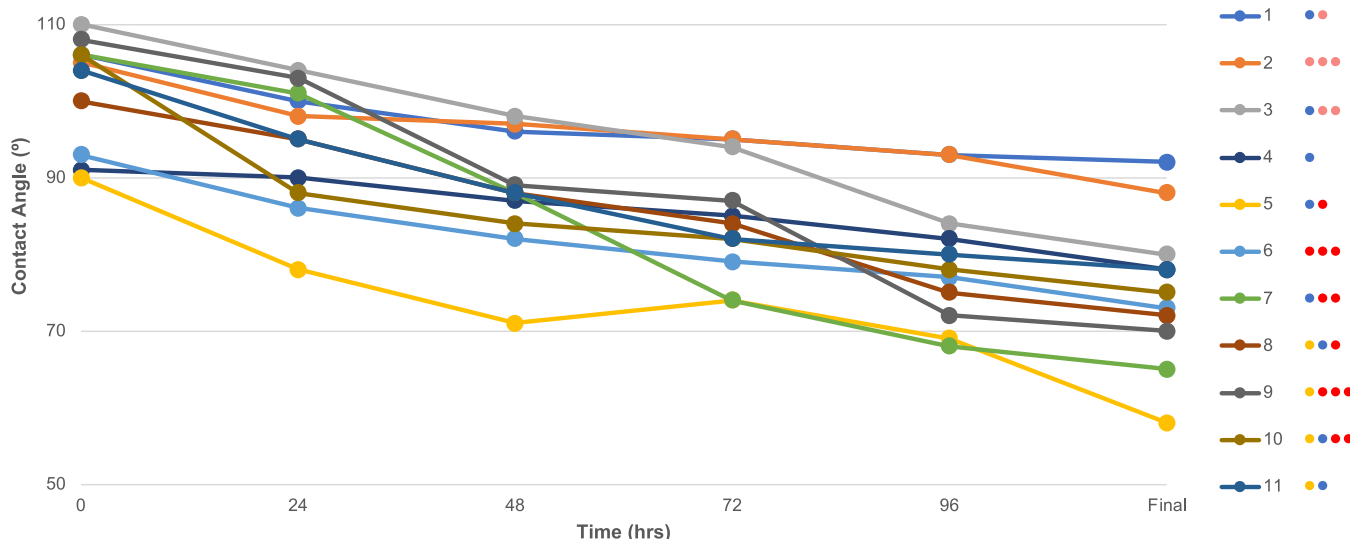


Figure 5. Captive bubble contact angles measured over a five-day period. All coatings show a drop in the contact angle, with coatings 5 and 7 showing the lowest final contact angles.

able to attach to surfaces more easily. Therefore, a fluorinated initiator, instead of a comonomer, was incorporated to determine its effect on the settlement of marine organisms.

Methacrylate monomers were chosen for their facile copolymerization via ATRP. Feed ratios of each comonomer relative to the initiator were selected to form terpolymers with targeted average number comonomer repeat units (Figures 3 and 4), and samples with number average molecular weights $M_n \approx 10,000 \text{ g mol}^{-1}$ were obtained (Figures S1 and S2). The amphiphilic components were provided by PEGMEMA and PDMSMA, known for their AF and FR properties, respectively. Various combinations of the PEG and PDMS functionalities have been used extensively in the past.¹² Block copolymers and random copolymers composed of PEG/PDMS moieties have displayed excellent AF and FR properties toward various microorganisms.^{19–23} Additionally, a range of the PTMA precursor component, PTMPM, was incorporated to find its effect on the AF and FR properties. The ratios between PEGMEMA and PDMSMA were kept the same to maintain the amphiphilic balance for all but one polymer per set, in which the hydrophilic PEGMEMA comonomer was not incorporated into the backbone, in order to elucidate the fouling-release properties of PTMA without PEGMEMA influence.

The results of polymerization are summarized in Figure S2. EBiB was an efficient initiator for all monomers. These polymers are used without any further modification as Set 1, the polymer amines. For easier readability, the sample IDs and colored labels, indicating their ratios as shown in Figure 3, shall be used henceforth. Although 17F-EBiB was a slower, less efficient initiator, with only about half of all monomer units polymerized, monomer ratios stayed consistent with their theoretical monomer unit ratios (Figure S2). Figures S3 and S4 show their respective ¹H NMR spectra, with important polymer peaks labeled. To obtain the nitroxide PTMA versions (Sets 2 and 3), both these polymers were subjected to oxidation, as described in the next section.

Oxidation to Nitroxide. Each polymer was oxidized to obtain the final TEMPO-containing terpolymers (Sets 2 and 3). Because precursor monomers were employed, it is important to optimize the amount of radical content on the

polymer backbone. The polymers are soluble in methanol, and we therefore employed a modified version of a previously reported recipe using $\text{H}_2\text{O}_2/\text{Na}_2\text{WO}_4$ as the oxidant to minimize overoxidation (which results in $^{\bullet}\text{N}=\text{O}$ moieties being present along the polymer backbone).⁴³ These experiments were complemented by electron paramagnetic resonance (EPR) spectroscopy to quantify the conversion and number of PTMA units in the final polymer. As illustrated in Figure S5, the reaction conditions were optimized using polymer 2 since it has the highest PTMPM content. The modified recipe successfully yielded ~70% functionalization in all the systems, which is similar to the literature value.⁴³ The reaction conditions for the best conversion are illustrated in Figure S5 along with their respective EPR spectra. As seen in the EPR spectra, the broadening of the EPR signal confirms that the signal is arising from polymeric PTMA. The FTIR spectra in Figure S5 clearly show the $\text{N}-\text{O}^{\bullet}$ signal at 1365 cm^{-1} , confirming the occurred reaction to PTMA, while the absence of the $^{\bullet}\text{N}=\text{O}$ signal at 1540 cm^{-1} indicates that there was no appreciable overoxidation, consistent with expectations for this oxidation mechanism.⁴³ The final ratios in the PEGMEMA-*r*-PTMA-*r*-PDMSMA polymer sets are represented in Figure 4. For easier readability, the sample IDs and colored labels indicate their ratios, as shown in Figure 4, shall be used henceforth.

Surface Characterization. The two-layer coatings were prepared using similar methods to those of a previous study with PDMS-based architecture, which produced polymers with mechanical properties conducive to effective fouling resistance.²⁰ First, an underlayer composed of PDMS with a cross-linker was spray cast on glass slides and annealed. Then, a second top layer comprising 4 wt % of chosen terpolymer in the same PDMS solution was spray cast and annealed. All the coatings were characterized by contact angle goniometry, AFM, and XPS. The films were submerged into water for 5 days to allow the polymer coatings to structurally reconstruct due to the media change at the polymer interface. Contact angle measurements give insight into the surface wettability and the film hydrophobicity. It is known that the surface hydrophobicity plays an important role in FR, and an optimal surface tension of $20\text{--}25 \text{ mN m}^{-1}$ has been found to be critical

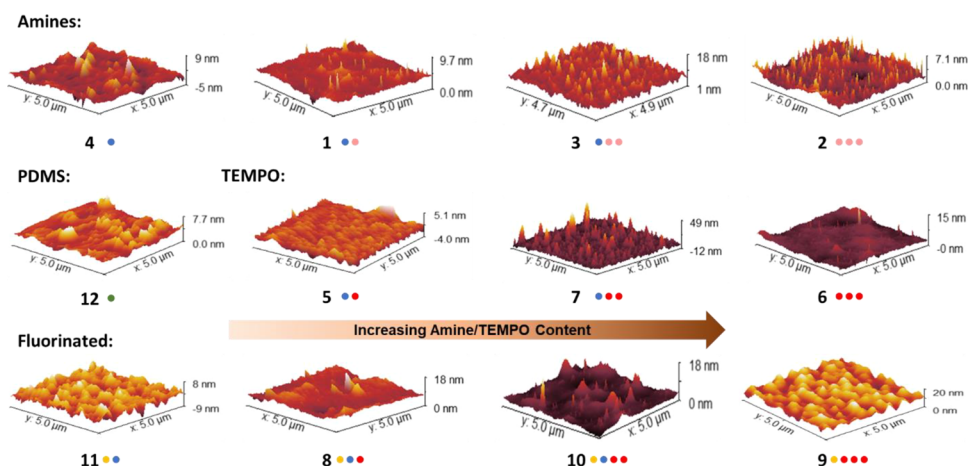


Figure 6. AFM images of coating surfaces after 7 days of immersion under water.

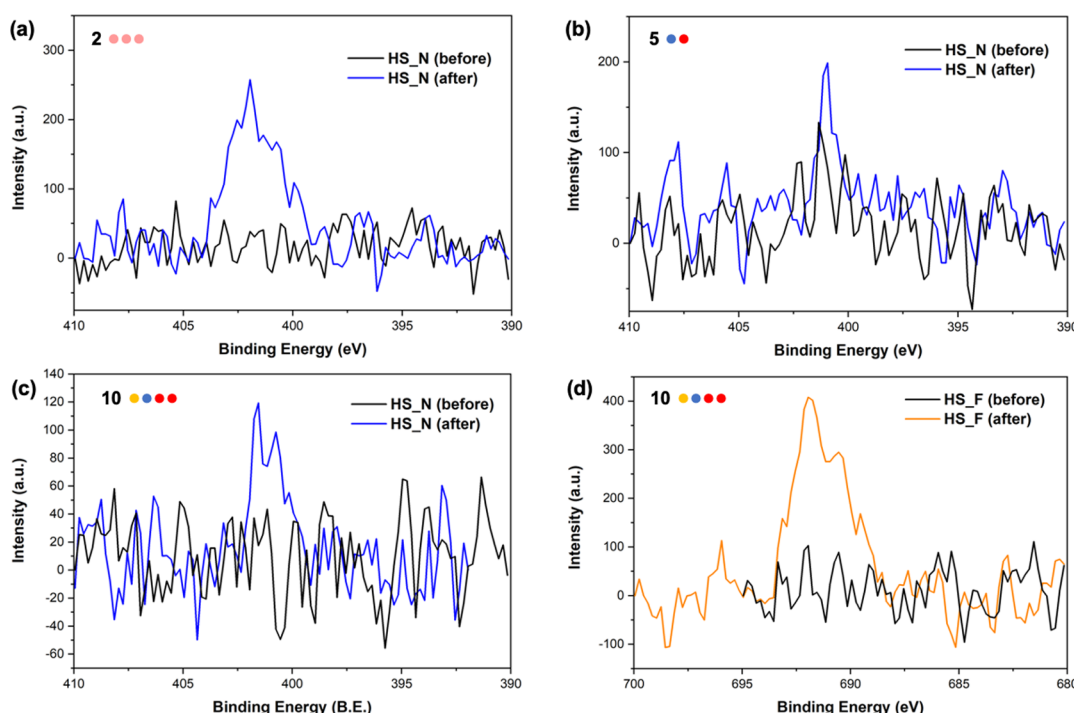
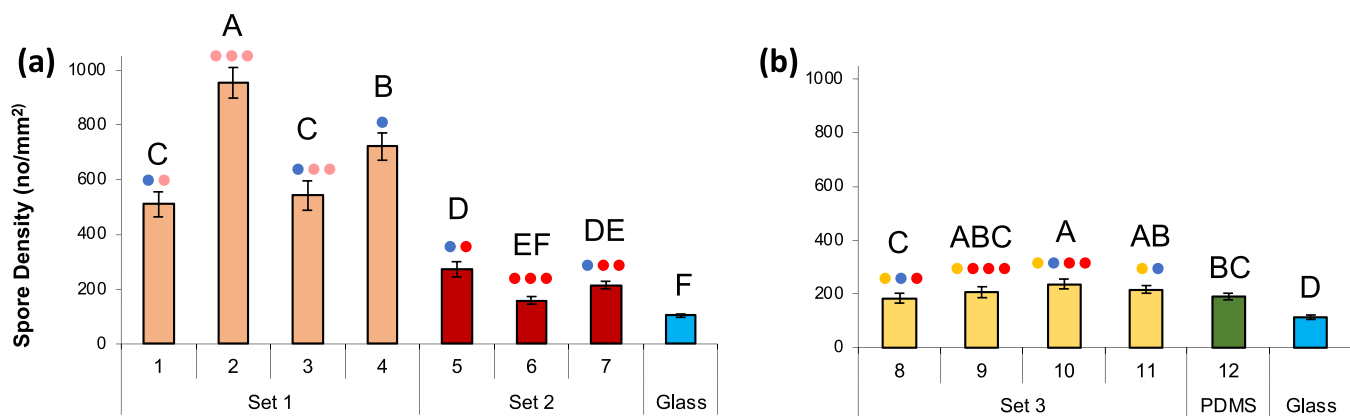


Figure 7. High-sensitivity XPS scans for N 1s in coatings made from (a) 2, (b) 5, (c) 10, and high sensitivity XPS scans for F 1s in coatings made from (d) 10; measured before (black line) and after immersion in water for 120 h (blue/orange line).

for their FR success against *N. incerta*, barnacles, and other organisms.¹² At the same time, however, amphiphilic balance is required to provide the optimal FR and AF properties. Captive bubble contact angle measurements of the films immersed in water were taken at 24 h intervals up to a period of 120 h. As seen from Figure 5, all the surfaces undergo rearrangement when immersed under water. The progressive and continuous decrease in the contact angle with immersion time was indicative of amphiphilicity due to an increase in surface hydrophilicity. The coatings typically took 5 days to reach a sort of minimal contact angle, that is maximal wetting, and therefore, this time period was applied to all our subsequent fouling assays. The initial contact angles θ of the coatings are all roughly around 100–110°, which is typical for PDMS.^{46,47} The amine polymers (Set 1) show low hydrophilicity with contact angles typically >90°. The coatings with both PEG and PTMA units had the lowest initial (~90°) and final contact

angles (58°–65°). It has been previously observed that having PEG units in the same polymer chain helps to pull TEMPO groups to the surface,³³ and this was consistent for these coatings as well. The coatings from the fluoro end-capped polymers had the highest initial contact angles (>105°) and final contact angles between 70°–80°. Overall, the coatings exhibited amphiphilic behavior. Values of θ for PDMS-based coatings composed of a surface-active, amphiphilic polymer additive such as those of the present work normally follow a decreasing trend with increasing immersion time in water. The rate of θ decrease depends on the character of the rearranging surface immersed in water, a more hydrophilic surface responding faster. A drop in θ may become apparent after up to 3-day or longer immersion time.^{29,44} Thus, the gradual drop in the contact angle observed here is in accordance with the previous literature and most likely a result of the very low 4 wt % loading of the functional terpolymer with randomized



U. linza settlement

Figure 8. Density of attached *U. linza* spores on stable radical coatings after 45 min settlement, run as two separate experiments. Each point is the mean from 90 counts on 3 replicate slides. Bars show 95% confidence limits. Statistical significance is generated from ANOVA and Tukey test, and bars that do not share the same letter are significantly different. Refer **Figures 3** and **4** for sample IDs and color labels.

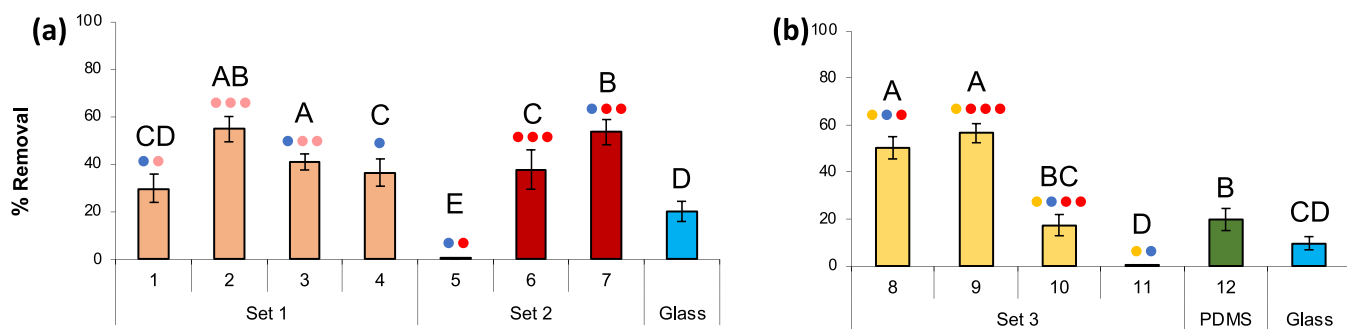
hydrophilic units in a largely hydrophobic PDMS matrix. The coatings containing both PEG and PTMA possessed the highest hydrophilicity of all the coatings, while the fluorinated coatings retained some hydrophobic characteristics even after immersion in water. In our work, here, we gained deeper insight into surface amphiphilicity features by studying modifications of the film surface before and after immersion in water by AFM and XPS (see below).

AFM was conducted to image the surface morphology of the coatings after immersion in water. Surface roughness plays a role in wettability, AF, and FR, with, for example, unicellular spores of *U. linza* preferentially settling on surfaces with roughness $>4 \mu\text{m}$. As seen from the AFM images in **Figure 6** and the roughness parameters in **Table S2**, the surface was very smooth for all the coatings, except coating 7, with R_q (RMS) $< 3 \text{ nm}$ and $R_z < 21 \text{ nm}$. As seen in **Figure 6**, the amines (Set 1) and the PTMA (Set 2) show sharp peaks which are most likely the amine/TEMPO clusters protruding from the surface. No such sharp peaks were observed in the coatings without amine/PTMA. The fluorinated copolymer coatings show larger features most likely arising from the segregation of the fluoro end-capped segment. A general trend in surface roughness has emerged, showing lower RMS for coatings with lower amine/TEMPO content, while the coatings with both PEG and amine/TEMPO showed the highest density and height of sharp peaks.

XPS measurements were carried out to elucidate the position of chemical moieties through the depth of the film. By incorporating the TEMPO functionality in increasing quantities, the surface properties and moieties are likely to be affected. Earlier work using polymer blends consisting of PEG and PTMA showed that TEMPO signals (via XPS) decreased after water exposure since PEG dominates the surface.³³ However, when the TEMPO functionality was attached to a PDMS backbone, TEMPO was much more prominent at the surface, especially when co-attached with PEG.³³ In our systems, it is expected that PTMA will segregate to the surface as it is incorporated as a terpolymer with hydrophilic (PEGMEMA) and low surface energy (PDMSMA) comonomers instead of a block copolymer. The XPS atomic percentages of C, O, Si, N, and F are listed in **Table S3**. It is important to note that the terpolymers are only loaded at 4 wt

% in a PDMS matrix, and as such, XPS is mostly dominated by Si and O. The rough trend shows that atomic % of Si and O decrease and atomic % of C increases marginally, indicative of increase in terpolymer concentration at the surface after immersion in water. This difference before and after immersion is greater for the fluorinated Set 3, indicating that the fluorinated segment assists segregation, pulling the terpolymer further out of the PDMS matrix. However, due to the low wt% of the terpolymer in the PDMS blend, any contribution from F 1s and N 1s is too low to be picked up in survey scans. Hence, high sensitivity XPS was conducted for N 1s and F 1s on the coatings before and after immersion in water. As seen in **Figure 7**, the N 1s signal is absent in the dry state but becomes evident after immersion in water. This is due to the surface rearrangement in water evidenced by the contact angle measurements shown earlier. As seen in the previous literature, after rearrangement, the amine/TEMPO groups segregate toward the surface.³³ The data in **Figure 7** are comparable with previously reported high sensitivity XPS data for coatings with such low loading percentages of the N-containing functional groups.²⁵ While higher numbers of co-attached PEG units are expected to more effectively pull the amine/PTMA groups to the surface, the final immersed state N 1s signal is still predominantly determined by the original amine/PTMA ratios. This observation seems to hold true even for the fluoro end-capped polymer coatings, with N 1s becoming visible after immersion in water (**Figure 7c**). The F 1s signal is also hidden in the dry state but becomes distinct after immersion in water (**Figure 7d**). Overall, the high sensitivity XPS results show that the copolymers are initially buried within the PDMS matrix in the as-cast state but segregate out of the PDMS bulk toward the surface upon immersion in water. This is enabled by the amphiphilic nature of the copolymer aided by the presence of hydrophilic PEG, amine, and PTMA components and further assisted by the incorporation of the fluorinated end block.

Fouling Studies. The three polymer sets were tested against a number of marine organisms. Three-layer coatings for biological assays were prepared according to a three-step procedure, as described in the **Experimental Section**. Related AF/FR PDMS-blend coatings containing amphiphilic copolymers have proven to be chemically stable and mechanically durable under laboratory bioassays and field immersion trials



U. linza removal

Figure 9. Removal of *U. linza* spores from the stable radical coatings due to exposure to a shear stress of 50 Pa, run as two separate experiments. Bars show 95% confidence limits derived from arc-sine transformed data. Statistical significance is generated from the ANOVA and Tukey test, and bars that do not share the same letter are significantly different. Refer [Figures 3 and 4](#) for sample IDs and color labels.

for several months.^{21,24,48,49} TEMPO has previously shown an ability to inhibit microbial growth. It was, therefore, of interest to test these materials against the settling stage of the alga *U. linza*, which produces spores which are only a little larger than bacteria (ca. 5–7 μm diameter). TEMPO has also exhibited a role in inhibiting barnacle settlement, which relies on radical-based cross-linking adhesives.³³ Another hard-fouler, the tubeworm *F. enigmaticus*, has also been included in our studies to determine if the PEG and TEMPO can exert an effect on organisms from other taxa. Finally, due to the low elastic modulus of the materials synthesized in this study, AF and FR results are expected to be an improvement on previous work.^{20,33}

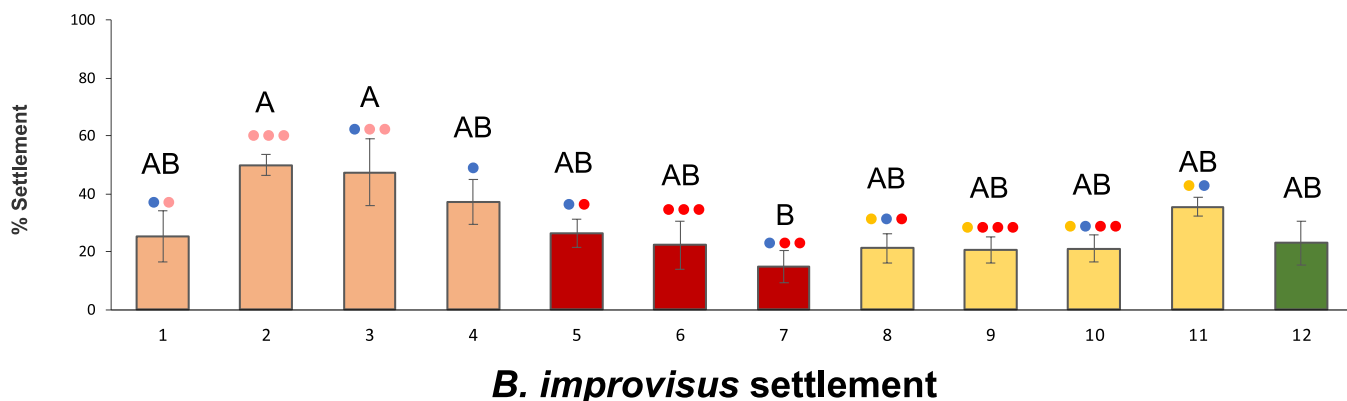
The control coating material used in these studies was PDMS which contained no stable radicals. Based on earlier work, it was expected that these samples would perform well (both with and without the fluorinated initiator) but that the response would vary between organisms.¹² Previous studies have revealed that long fluoroalkyl chains aid in inhibiting barnacle settlement.¹⁹ Therefore, it would be interesting to compare the results between copolymers with no TEMPO incorporation on barnacle antifouling. No improvements, however, have been seen between *Ulva* settlement with the incorporation of fluorine.⁵⁰ Differences between coatings were tested using a one-way analysis of variance (ANOVA) followed by the Tukey test in the assays with the alga and the barnacle, and by PERMANOVA followed by the Monte Carlo post-test in the assay with the tubeworm.

U. Linza. Previously, *U. linza* settlement studies using similar methacrylate polymer coatings blended with PDMS had all incurred greater settlement than the bare PDMS control.²⁰ Within the coatings in this study, spore settlement densities were higher on the coatings of amine polymers Set 1, which lacked TEMPO, than from Set 2 which contained TEMPO (one-way ANOVA and Tukey test F 7, 712 = 232 $p < 0.05$) ([Figure 8](#)). The settlement values for set 3 were also considerably lower than those from Set 1. However, in the case of these coatings, settlement on the control coating 11 without TEMPO was also low (one way ANOVA and Tukey test F 5, 534 = 28.7 $p < 0.05$) (Statistical analysis for the settlement data is reported in full in [Figure 8](#) and [Table S5](#)). Importantly, the settlement densities for Sets 2 and 3 are comparable to the PDMS control. Those for Set 1, although higher, are still a third of those reported in the previous literature with similar methacrylate polymer systems,²⁰ most likely resulting from the

modified architecture of the polymers. The previous study had PDMS as an end-cap block, while this system has PDMSMA as a random copolymer component. This aids assimilation within the PDMS matrix, preserves more of the hydrophobic aspect of PDMS at the surface, and generates truly amphiphilic “ambiguous” surfaces. The high spore settlement densities on Set 1 caused the spores to aggregate in clumps. While *U. linza* settles preferentially on rough surfaces, the length scales of roughness for all these coatings were well below the critical value of 10 μm above which roughness becomes a factor.⁵¹ Hence, the differences in *U. linza* settlement on these coatings clearly arise from surface chemistry of the various components. The settlement was the lowest on the coating 6 containing only TEMPO. Whether the radical properties of the TEMPO affected the settlement of spores, for example, by disrupting the spore surface sensing mechanisms, or whether the presence of the TEMPO changed some other properties of the coating surface cannot be discerned at this time.

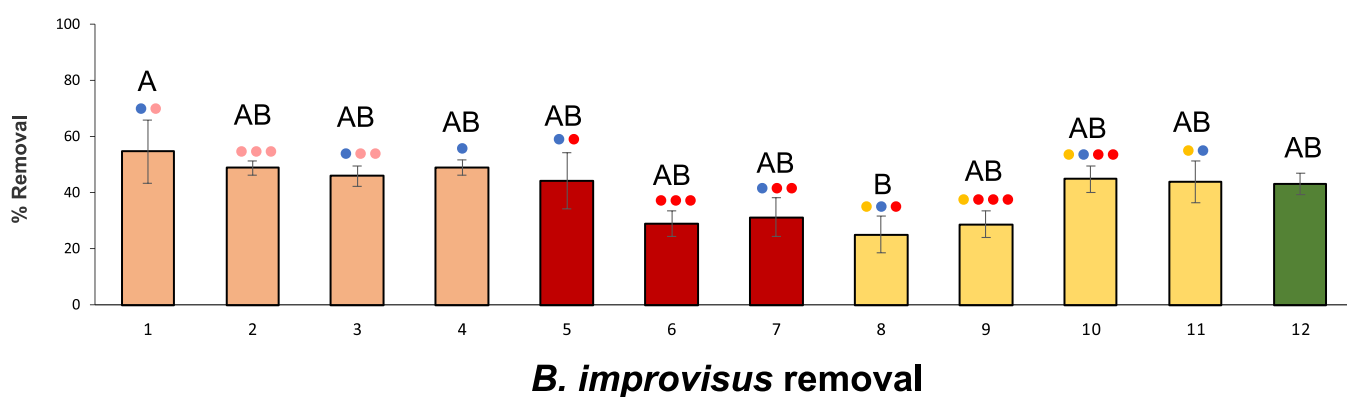
U. linza removal data, as seen in [Figure 9](#) and [Table S5](#), show that spore removal from Set 1, which lacked TEMPO, varied between 30 and 55%. In Set 2, the two coatings with the highest TEMPO content had removal levels of 38 and 54%, which was similar in magnitude to removal from Set 1, and indicated that the incorporation of the radical did not aid ease of removal of spores (one-way ANOVA and Tukey test F 7, 712 = 46.95 $p < 0.05$). However, the presence of TEMPO above a threshold seemed to assist removal, as coatings with only a low TEMPO content, such a coating 5, had negligible removal. Coating 7, containing both TEMPO and PEG, had the highest removal. In Set 3, the highest levels of removal, 50 and 57%, were also comparable to those from the other sets. However, in the case of Set 3, the trend in removal was proportional to the content of TEMPO in the coating (one-way ANOVA and Tukey test F 5, 534 = 87.3 $p < 0.05$). Removal from the PDMS matrix alone was substantially lower than that from most of the formulations. Compared to the previous literature on PS-PDMS coating systems containing TEMPO,³³ in which fouling release efficiency was lower than the control and only marginally better than glass, this current system shows a significant improvement. In the case of Set 3, it has successfully delivered TEMPO to the surface of a nanoscalar amphiphilic ambiguous surface and brought about the release of spores of *U. linza*.

The radical action of TEMPO was more likely to affect the adhesion strength of the spores rather than their settlement. In



B. improvisus settlement

Figure 10. Percent settlement of 3-day old *B. improvisus* cyprids on the test coatings after 72 h. Mean from 6 replicates is shown with error bars showing 95% confidence limits derived from arc-sine transformed data. Letters show significantly similar coatings based on the one-way ANOVA and Tukey test. Refer Figures 3 and 4 for sample IDs and color labels.



B. improvisus removal

Figure 11. Percent removal of *B. improvisus* barnacles from test coatings. Bars show mean from 6 replicate coatings with error bars showing 95% confidence limits derived from arc-sine transformed data. Letters show significantly similar coatings based on one-way ANOVA and the Tukey test. Refer Figures 3 and 4 for sample IDs and color labels.

Set 2 and 3, the removal of spores did not increase due to the incorporation of TEMPO. However, in Set 3, the level of removal was proportional to the content of TEMPO, falling to zero when the TEMPO was absent. Since the physical surface properties of these coatings are all very similar, it is likely that the TEMPO itself was directly affecting adhesion strength. In general, the inclusion of TEMPO reduced settlement densities and in Set 3, in which the copolymer was end-capped with a fluoro group, appeared to drive removal.

The density of spores remaining on the coatings after exposure to the shear stress is shown in Figure S6 and Table S5. Overall, PEG, TEMPO, and the fluoro end-block all contributed to improving fouling resistance with coating 8 exhibiting the lowest final spore density. Across both Sets 2 and 3, the coatings 6 and 9 with TEMPO but without PEG perform extremely well and were comparable to coatings 7 and 8 with co-attached PEG. Important to note here that the coatings 6 and 7 have higher TEMPO contents than coatings 7 and 8 with TEMPO + PEG. In this study, TEMPO is clearly the dominant functionality affecting fouling resistance against the *U. linza*. As such, while the ambiguity of coatings 7 and 8 definitely make them effective, they are matched by coatings 6 and 7 due to their higher TEMPO content. These are interesting results and a longer-term study in which the contact time between the plant and radical would be extended (days not hours), such as using sporelings rather than spores, might show more activity from the TEMPO. However, this has to be

set against the possibility that interactions with compounds present in seawater might reduce the activity of the radical and limit its effectiveness.

B. improvisus. The duration of the settlement assay was 72 h. Counts of settled and unsettled barnacles were made and the percentage attached was recorded. The mean percent settlement from 6 replicate slides is shown in Figure 10. One-way ANOVA ($F_{11, 60} = 2.6$ $p < 0.05$) with the Tukey test showed that the only significant difference was between coatings 2 and 3 against coating 7 (Table S5). However, the trend indicated higher settlement density on all the coatings in Set 1 compared to the coatings in Sets 2 and 3 that contained TEMPO. Even among Set 1 coatings with the amines, the coatings with low amine content or higher relative PEG content performed better, clearly indicating that the amines actively promote settlement. Settlement was the lowest on coating 7 with both TEMPO and PEG. Coating 11 from Set 3 contained no TEMPO and also had a higher settlement density, clearly indicating the importance of the TEMPO functionality. In previous reports with PS-PDMS based systems, certain TEMPO-based coatings inhibited barnacle settlement completely, albeit the TEMPO content in the surface active layer was closer to 20%.³³ Comparatively, in the current system, the TEMPO content is $\sim 2\%$ for all the coatings and notably $\sim 1\%$ in the coatings with co-attached PEG. In light of this, the observed inhibition of barnacle settlement is extremely promising and warrants further

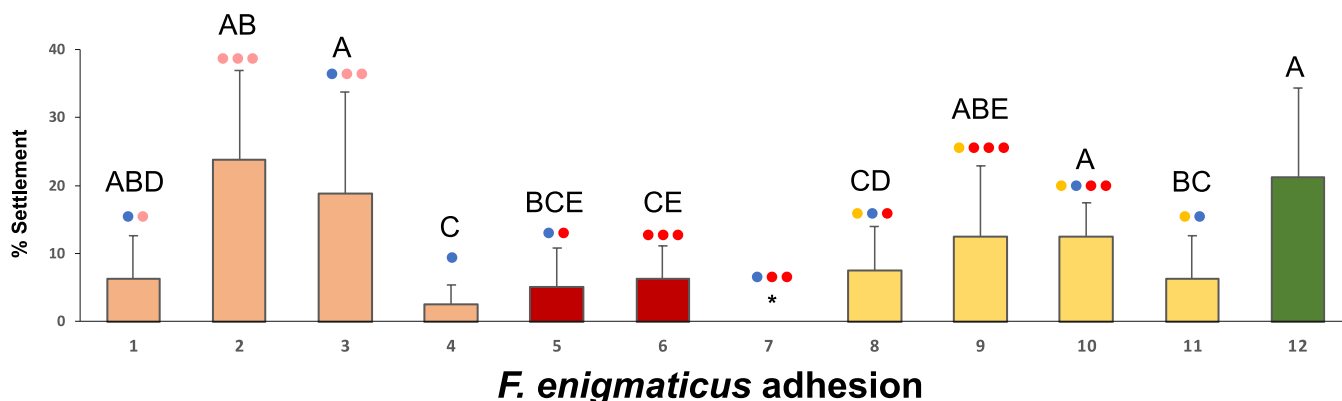


Figure 12. Mean percentage of *F. enigmatus* larval settlement on different surface samples, after 5 days of exposure. Initial number of larvae = 20. PERMANOVA analysis ($n = 6$), followed by Monte Carlo post-test, was performed for all coatings. Not-shared letters indicate statistically significant differences, $p \leq 0.05$. Refer Figures 3 and 4 for sample IDs and color labels.

exploration of this system with higher wt % loading of the terpolymer.

Previous reports have demonstrated the strong ability of TEMPO to interfere with barnacle adhesion.³³ At the time of testing for the current study, the juvenile barnacles were 6 days old. The percentage removal due to exposure to a water jet was recorded. The mean percent removal from 6 replicate slides is shown in Figure 11. The total number of barnacles tested is listed in Table S4. It is noteworthy that these numbers broadly correspond to the percent settlement data in Figure 10. One-way ANOVA ($F_{10,55} = 2.7$ $p < 0.05$) with the Tukey test showed that the only significant difference in removal was between coating 1 and coating 8 (Table S5). Although not statistically significant, coatings 6, 7, 8, and 9 had distinctly lower removal than the other coatings. Removal levels from the TEMPO-containing coatings 5, 9, and 10 were similar to those from set 1 that lacked TEMPO. Thus, the amines show greater removal, which might also be influenced by the fact that they had much higher settlement. However, the highest removal was observed for coating 1, which incidentally showed the lowest settlement within Set 1. For Sets 2 and 3, the coatings with both PEG and TEMPO showed better removal, albeit at different relative ratios (coating 5 for Set 2 and coating 10 for Set 3).

The attachment density of cyprids was higher on the coatings lacking TEMPO (i.e., coating Set 1 and coating 11 of Set 3) than on those containing TEMPO (Sets 2 and 3). Although this is not statistically significant, a trend can be seen. In line with this result, more barnacles remain settled on Set 1 in the removal assay than on most of the other coatings (see Figures 10 and 11). The removal of barnacles was not increased by the presence of TEMPO. Rather, removal was lower from four of the TEMPO-containing coatings than from the coatings in which it was absent. Overall, coating 7 from Set 2, containing both TEMPO and PEG, with its low settlement and good removal, was among the most effective coatings against the barnacles, only bettered marginally by coating 10 from Set 3, which contained the same component ratio with an additional fluoro end-cap.

F. enigmatus. In this study, we begin to explore TEMPO effectiveness against the marine tubeworm *Ficopomatus enigmatus*.^{36,47,52,53} The antioxidant mechanism of the nitroxide radical which inhibits barnacle adhesives is expected to translate to these marine tubeworms which use L-DOPA for attachment and metamorphosis.^{54–57} As one can see with the

F. enigmatus settlement assays in Figure 12, the amines showed high percent of settled larvae, which increased with increasing amine content (Table S6). The TEMPO once again proved to be a more effective functional group than the amines in reducing larval settlement. In all the sets, the coating with just amine/TEMPO performed the worst, which suggests that the TEMPO is only effective against *F. enigmatus* in the presence of PEG. In fact, the larval settlement was greatly reduced whenever TEMPO was combined with PEG. In general, PEG appeared to be the most important functionality for reducing the *F. enigmatus* larval settlement across all sets. The superior performance of hydrophilic PEG in the removal of *F. enigmatus* has been previously reported in similar systems, and these results show improvements in inhibiting settlement as well.⁴⁷ Even for the amines which have settlement comparable to the control, the samples with higher relative PEG content show significantly lower settlement. The importance of hydrophilicity for reducing *F. enigmatus* larval settlement warrants additional studies with longer PEG chains. Overall, the best performing coating was 7, which contained both TEMPO and PEG, for which no adhesion was observed, making it a near-perfect antifouling coating for this species. Across all ratios, the fluoro end-capped set clearly performed worse than Set 2, but the same trend with TEMPO alone being the worst and TEMPO+PEG being better was maintained. The increase in *F. enigmatus* larval settlement with fluorinated coatings adds to previous reports of lower removal from similar fluorinated systems.⁴⁷ Importantly, in this study, we identify the additional improvement that is afforded by co-attaching PEG with TEMPO.

CONCLUSIONS

The article describes the synthesis of random terpolymers composed of polymethacrylates of PEG, TEMPO, and PDMS, obtained via facile ATRP methods. Polymers with the amine precursor PTMPM were initially synthesized and later converted to the radical PTMA (TEMPO) counterparts. In addition, a fluoro end-capped set was also synthesized using similar methods. The individual and comparative effects of each group have been studied for antifouling and fouling-release efficacy against three marine foulers, *U. linza*, *B. improvisus*, and *F. enigmatus*.

Across all the coatings, the precursor amine set, hypothesized to work as a double anti-oxidant, instead promoted settlement for all the foulers, confirming previous reports of

high fouler affinity of amines. Against *U. linza*, the copolymers containing TEMPO were found to be extremely efficient at inhibiting settlement and significantly improved release compared to previous studies, especially when co-attached with PEG and the fluorinated end-block. Incorporation of the fluorinated end block and PEG into the polymer on their own did not improve spore release, but in conjunction with TEMPO, there was a marked improvement. While the mechanism for TEMPO against *U. linza* is not yet understood fully, its effectiveness has been established in this study. Against the barnacle *B. improvisus*, coating 7, containing co-attached PEG and TEMPO, once again demonstrated the best combination of settlement inhibition and removal, and was bettered only marginally by the fluorinated version of the same composition. The likely reason for this marginal improvement was that the presence of the fluorinated groups retained the TEMPO groups closer to the coating surface, ensuring a more uniform coverage.

On exploring the efficacy of these functionalities against the rarely studied serpulid *F. enigmaticus*, once again, coating 7 was the best composition, completely inhibiting settlement, making it a highly effective barrier against this species of tubeworm. Fluorination was found to increase the larval settlement of *F. enigmaticus* across all compositions. The surface expression contribution of the fluorinated groups marginally helped against the barnacles likely being outweighed by their hydrophobic character against the tubeworms which have consistently showed a strong dislike for predominantly hydrophilic coatings.

Importantly, in the search for broad-spectrum materials capable of resisting multiple types of marine foulers, coating 7 with a PEG–TEMPO ratio of 7:17, and no fluorinated end-block, has emerged as the most promising combination with high effectiveness against all three types of foulers. Even at the very low loading of 4 wt % within a PDMS blend, these coatings demonstrated observable improvements in broad-spectrum fouling resistance, warranting further exploration at higher loading percentages and over longer durations, to create a new generation of truly amphiphilic “ambiguous” fouling-resistant coatings.

ASSOCIATED CONTENT

Supporting Information

The Supporting Information is available free of charge at <https://pubs.acs.org/doi/10.1021/acsami.2c23213>.

Details of surface characterization methods; GPC and ¹H NMR characterization data for the copolymers; reaction scheme for oxidation to PTMA; EPR and FTIR characterization of the PTMA polymers; roughness measurements from AFM; complete XPS surface compositions; and additional fouling assay data with Tukey Test variance statistics ([PDF](#))

AUTHOR INFORMATION

Corresponding Authors

Elisa Martinelli – Dipartimento di Chimica e Chimica Industriale, Università di Pisa, Pisa 56124, Italy;
Email: elisa.martinelli@unipi.it

Christopher K. Ober – Department of Materials Science and Engineering, Cornell University, Ithaca, New York 14853, United States; [orcid.org/0000-0002-3805-3314](#);
Email: cko3@cornell.edu

Authors

Riddhiman Medhi – Department of Materials Science and Engineering, Cornell University, Ithaca, New York 14853, United States; [orcid.org/0000-0002-2368-2468](#)

Alicia Cintora – Department of Materials Science and Engineering, Cornell University, Ithaca, New York 14853, United States

Elisa Guazzelli – Dipartimento di Chimica e Chimica Industriale, Università di Pisa, Pisa 56124, Italy; [orcid.org/0000-0003-2884-3053](#)

Nila Narayan – Department of Materials Science and Engineering, Cornell University, Ithaca, New York 14853, United States

Amanda K. Leonardi – Department of Materials Science and Engineering, Cornell University, Ithaca, New York 14853, United States

Giancarlo Galli – Dipartimento di Chimica e Chimica Industriale, Università di Pisa, Pisa 56124, Italy

Matteo Oliva – Consorzio Interuniversitario di Biologia Marina e Ecologia Applicata “G. Bacci”, Livorno 57128, Italy; [orcid.org/0000-0002-0008-0827](#)

Carlo Pretti – Consorzio Interuniversitario di Biologia Marina e Ecologia Applicata “G. Bacci”, Livorno 57128, Italy; Dipartimento di Scienze Veterinarie, Università di Pisa, Pisa 56124, Italy

John A. Finlay – School of Natural and Environmental Sciences, Newcastle University, Newcastle upon Tyne NE1 7RU, U.K.

Anthony S. Clare – School of Natural and Environmental Sciences, Newcastle University, Newcastle upon Tyne NE1 7RU, U.K.

Complete contact information is available at: <https://pubs.acs.org/10.1021/acsami.2c23213>

Author Contributions

△R.M. and A.C. contributed equally to this research. R.M. and A.C. contributed equally to this research with contributions in polymer design, synthesis, coating preparation, and surface characterization; N.N. contributed to coating preparation and surface characterization; A.K.L. and C.K.O. contributed to polymer and experiment design; E.G., G.G., M.O., C.P., and E.M. contributed to coating preparation and *F. enigmaticus* assays; J.A.F. and A.S.C. contributed to *U. linza* and *B. improvisus* assays. The manuscript was written through contributions of all authors. All authors have given approval to the final version of the manuscript.

Notes

The authors declare no competing financial interest.

ACKNOWLEDGMENTS

This research was primarily supported by the Office of Naval Research awards N000141612960 and N000142012248. This work made use of the Cornell Center for Materials Research Shared Facilities which are supported through the NSF MRSEC program (DMR-1719875). This work made use of the Cornell University NMR Facility, which is supported, in part, by the NSF through MRI award CHE-1531632.

REFERENCES

- (1) Lejars, M.; Margaillan, A.; Bressy, C. Fouling Release Coatings: A Nontoxic Alternative to Biocidal Antifouling Coatings. *Chem. Rev.* **2012**, *112*, 4347–4390.

(2) Roberts, D.; Rittschof, D.; Holm, E.; Schmidt, A. R. Factors Influencing Initial Larval Settlement: Temporal, Spatial and Surface Molecular Components. *J. Exp. Mar. Biol. Ecol.* **1991**, *150*, 203–221.

(3) Clare, A. S.; Rittschof, D.; Gerhart, D. J.; Maki, J. S. Molecular Approaches to Nontoxic Antifouling. *Invertebr. Reprod. Dev.* **1992**, *22*, 67–76.

(4) Yu, M.; Hwang, J.; Deming, T. J. Role of 1,3-Dihydroxyphenylalanine in Mussel Adhesive Proteins. *J. Am. Chem. Soc.* **1999**, *121*, 5825–5826.

(5) Huang, K.; Lee, B. P.; Ingram, D. R.; Messersmith, P. B. Synthesis and Characterization of Self-Assembling Block Copolymers Containing Bioadhesive End Groups. *Biomacromolecules* **2002**, *3*, 397–406.

(6) Waite, J. H. Mussel Adhesion – Essential Footwork. *J. Exp. Biol.* **2017**, *220*, 517–530.

(7) Kamino, K.; Inoue, K.; Maruyama, T.; Takamatsu, N.; Harayama, S.; Shizuri, Y. Barnacle Cement Proteins: Importance of Disulfide Bonds in their Insolubility. *J. Biol. Chem.* **2000**, *275*, 27360–27365.

(8) So, C. R.; Scancella, J. M.; Fears, K. P.; Esock-Burns, T.; Haynes, S. E.; Leary, D. H.; Diana, Z.; Wang, C.; North, S.; Oh, C. S.; Wang, Z.; Orihuela, B.; Rittschof, D.; Spillmann, C. M.; Wahl, K. J. Oxidase Activity of the Barnacle Adhesive Interface Involves Peroxide-Dependent Catechol Oxidase and Lysyl Oxidase Enzymes. *ACS Appl. Mater. Interfaces* **2017**, *9*, 11493–11505.

(9) Fears, K. P.; Orihuela, B.; Rittschof, D.; Wahl, K. J. Acorn Barnacles Secrete Phase-Separating Fluid to Clear Surfaces Ahead of Cement Deposition. *Adv. Sci.* **2018**, *5*, No. 1700762.

(10) Corbett, J. J.; Koehler, H. W. Updated Emissions from Ocean Shipping. *J. Geophys. Res. Atmos.* **2003**, *108*, 4650.

(11) Davidson, I.; Scianni, C.; Hewitt, C.; Everett, R.; Holm, E.; Tamburri, M.; Ruiz, G. Mini-Review: Assessing the Drivers of Ship Biofouling Management – Aligning Industry and Biosecurity Goals. *Biofouling* **2016**, *32*, 411–428.

(12) Leonardi, A. K.; Ober, C. K. Polymer-Based Marine Antifouling and Fouling Release Surfaces: Strategies for Synthesis and Modification. *Annu. Rev. Chem. Biomol. Eng.* **2019**, *10*, 241–264.

(13) Baier, R. E. Surface Behaviour of Biomaterials: The Theta Surface for Biocompatibility. *J. Mater. Sci.: Mater. Med.* **2006**, *17*, 1057.

(14) St. Hill, L. R.; Craft, J. W.; Chinwangso, P.; Tran, H.-V.; Marquez, M. D.; Lee, T. R. Antifouling Coatings Generated from Unsymmetrical Partially Fluorinated Spiroalkanedithiols. *ACS Appl. Bio Mater.* **2021**, *4*, 1563–1572.

(15) Ma, J.; Porath, L. E.; Haque, M. F.; Sett, S.; Rabbi, K. F.; Nam, S.; Miljkovic, N.; Evans, C. M. Ultra-Thin Self-Healing Vitrimer Coatings for Durable Hydrophobicity. *Nat. Commun.* **2021**, *12*, 5210.

(16) Prime, K. L.; Whitesides, G. M. Adsorption of Proteins onto Surfaces Containing End-Attached Oligo(ethylene oxide): A Model System using Self-Assembled Monolayers. *J. Am. Chem. Soc.* **1993**, *115*, 10714–10721.

(17) Ekblad, T.; Bergström, G.; Ederth, T.; Conlan, S. L.; Mutton, R.; Clare, A. S.; Wang, S.; Liu, Y.; Zhao, Q.; D’Souza, F.; Donnelly, G. T.; Willemse, P. R.; Pettitt, M. E.; Callow, M. E.; Callow, J. A.; Liedberg, B. Poly(ethylene glycol)-Containing Hydrogel Surfaces for Antifouling Applications in Marine and Freshwater Environments. *Biomacromolecules* **2008**, *9*, 2775–2783.

(18) Yang, W. J.; Pranantyo, D.; Neoh, K.-G.; Kang, E.-T.; Teo, S. L.-M.; Rittschof, D. Layer-by-Layer Click Deposition of Functional Polymer Coatings for Combating Marine Biofouling. *Biomacromolecules* **2012**, *13*, 2769–2780.

(19) Oliva, M.; Martinelli, E.; Galli, G.; Pretti, C. PDMS-Based Films Containing Surface-Active Amphiphilic Block Copolymers to Combat Fouling from Barnacles *B. amphitrite* and *B. improvisus*. *Polymer* **2017**, *108*, 476–482.

(20) Wenning, B. M.; Martinelli, E.; Mieszkin, S.; Finlay, J. A.; Fischer, D.; Callow, J. A.; Callow, M. E.; Leonardi, A. K.; Ober, C. K.; Galli, G. Model Amphiphilic Block Copolymers with Tailored Molecular Weight and Composition in PDMS-Based Films to Limit Soft Biofouling. *ACS Appl. Mater. Interfaces* **2017**, *9*, 16505–16516.

(21) Martinelli, E.; Sarvothaman, M. K.; Alderighi, M.; Galli, G.; Mielczarski, E.; Mielczarski, J. A. PDMS Network Blends of Amphiphilic Acrylic Copolymers with Poly(ethylene glycol)-Fluoroalkyl Side Chains for Fouling-Release Coatings. I. Chemistry and Stability of the Film Surface. *J. Polym. Sci., Part A: Polym. Chem.* **2012**, *50*, 2677–2686.

(22) Martinelli, E.; Suffredini, M.; Galli, G.; Glisenti, A.; Pettitt, M. E.; Callow, M. E.; Callow, J. A.; Williams, D.; Lyall, G. Amphiphilic Block Copolymer/Poly(dimethylsiloxane) (PDMS) Blends and Nanocomposites for Improved Fouling-Release. *Biofouling* **2011**, *27*, 529–541.

(23) Galli, G.; Barsi, D.; Martinelli, E.; Glisenti, A.; Finlay, J. A.; Callow, M. E.; Callow, J. A. Copolymer Films Containing Amphiphilic Side Chains of Well-Defined Fluoroalkyl-Segment Length with Biofouling-Release Potential. *RSC Adv.* **2016**, *6*, 67127–67135.

(24) Guazzelli, E.; Perondi, F.; Criscitiello, F.; Pretti, C.; Oliva, M.; Casu, V.; Maniero, F.; Gazzera, L.; Galli, G.; Martinelli, E. New Amphiphilic Copolymers for PDMS-Based Nanocomposite Films with Long-Term Marine Antifouling Performance. *J. Mater. Chem. B* **2020**, *8*, 9764–9776.

(25) Leonardi, A. K.; Medhi, R.; Zhang, A.; Düzen, N.; Finlay, J. A.; Clarke, J. L.; Clare, A. S.; Ober, C. K. Investigation of N-Substituted Morpholine Structures in an Amphiphilic PDMS-Based Antifouling and Fouling-Release Coating. *Biomacromolecules* **2022**, *23*, 2697–2712.

(26) Martinelli, E.; Del Moro, I.; Galli, G.; Barbaglia, M.; Bibbiani, C.; Mennillo, E.; Oliva, M.; Pretti, C.; Antonioli, D.; Laus, M. Photopolymerized Network Polysiloxane Films with Dangling Hydrophilic/Hydrophobic Chains for the Biofouling Release of Invasive Marine Serpulid *Ficopomatus enigmaticus*. *ACS Appl. Mater. Interfaces* **2015**, *7*, 8293–8301.

(27) Poláková, L.; Raus, V.; Kostka, L.; Braunová, A.; Pilař, J.; Lobaz, V.; Pánek, J.; Sedláková, Z. Antioxidant Properties of 2-Hydroxyethyl Methacrylate-Based Copolymers with Incorporated Sterically Hindered Amine. *Biomacromolecules* **2015**, *16*, 2726–2734.

(28) Poláková, L.; Raus, V.; Cuchalová, L.; Poręba, R.; Hrubý, M.; Kučka, J.; Větvička, D.; Trhlíková, O.; Sedláková, Z. SHARP Hydrogel for the Treatment of Inflammatory Bowel Disease. *Int. J. Pharm.* **2022**, *613*, No. 121392.

(29) Alexander, Rouse, E. M.; White, J. M.; Tse, N.; Kyi, C.; Schiesser, C. H. Controlling Biofilms on Cultural Materials: the Role of 3-(dodecane-1-thiyl)-4-(hydroxymethyl)-2,2,5,5-tetramethyl-1-pyrrolinoyl. *Chem. Commun.* **2015**, *51*, 3355–3358.

(30) Alexander, S.-A.; Kyi, C.; Schiesser, C. H. Nitroxides as Anti-Biofilm Compounds for the Treatment of *Pseudomonas aeruginosa* and Mixed-Culture Biofilms. *Org. Biomol. Chem.* **2015**, *13*, 4751–4759.

(31) de la Fuente-Núñez, C.; Reffuveille, F.; Fairfull-Smith Kathryn, E.; Hancock Robert, E. W. Effect of Nitroxides on Swarming Motility and Biofilm Formation, Multicellular Behaviors in *Pseudomonas aeruginosa*. *Antimicrob. Agents Chemother.* **2013**, *57*, 4877–4881.

(32) Boase, N. R. B.; Torres, M. D. T.; Fletcher, N. L.; de la Fuente-Núñez, C.; Fairfull-Smith, K. E.; Fairfull-Smith, K. E. Polynitroxide Copolymers to Reduce Biofilm Fouling on Surfaces. *Polym. Chem.* **2018**, *9*, 5308–5318.

(33) Leonardi, A.; Zhang, A. C.; Düzen, N.; Aldred, N.; Finlay, J. A.; Clarke, J. L.; Clare, A. S.; Segalman, R. A.; Ober, C. K. Amphiphilic Nitroxide-Bearing Siloxane-Based Block Copolymer Coatings for Enhanced Marine Fouling Release. *ACS Appl. Mater. Interfaces* **2021**, *13*, 28790–28801.

(34) Patterson, A. L.; Wenning, B.; Rizis, G.; Calabrese, D. R.; Finlay, J. A.; Franco, S. C.; Zuckermann, R. N.; Clare, A. S.; Kramer, E. J.; Ober, C. K.; Segalman, R. A. Role of Backbone Chemistry and Monomer Sequence in Amphiphilic Oligopeptide- and Oligopeptoid-Functionalized PDMS- and PEO-Based Block Copolymers for Marine Antifouling and Fouling Release Coatings. *Macromolecules* **2017**, *50*, 2656–2667.

(35) Gudipati, C. S.; Finlay, J. A.; Callow, J. A.; Callow, M. E.; Wooley, K. L. The Antifouling and Fouling-Release Performance of Hyperbranched Fluoropolymer (HBFP)-Poly(ethylene glycol) (PEG) Composite Coatings Evaluated by Adsorption of Biomacromolecules and the Green Fouling Alga *Ulva*. *Langmuir* **2005**, *21*, 3044–3053.

(36) De Marchi, L.; Pretti, C.; Cuccaro, A.; Oliva, M.; Tardelli, F.; Monni, G.; Magri, M.; Bulleri, F. A Multi-Bioassay Integrated Approach to Assess Antifouling Potential of Extracts from the Mediterranean Sponge *Ircinia oros*. *Environ. Sci. Pollut. Res.* **2022**, *29*, 1521–1531.

(37) Rodriguez, L. F. Can Invasive Species Facilitate Native Species? Evidence of How, When, and Why These Impacts Occur. *Biol. Invasions* **2006**, *8*, 927–939.

(38) Gabilondo, R.; Graham, H.; Caldwell, G. S.; Clare, A. S. Laboratory Culture and Evaluation of the Tubeworm *Ficopomatus enigmaticus* for Biofouling Studies. *Biofouling* **2013**, *29*, 869–878.

(39) Göbel, B.; Matyjaszewski, K. Diimino- and Diaminopyridine Complexes of CuBr and FeBr₂ as Catalysts in Atom Transfer Radical Polymerization (ATRP). *Macromol. Chem. Phys.* **2000**, *201*, 1619–1624.

(40) Kyeremateng, S. O.; Busse, K.; Kohlbrecher, J.; Kressler, J. Synthesis and Self-Organization of Poly(propylene oxide)-Based Amphiphilic and Triphilic Block Copolymers. *Macromolecules* **2011**, *44*, 583–593.

(41) Perrier, S.; Jackson, S. G.; Haddleton, D. M.; Améduri, B.; Boutevin, B. Preparation of Fluorinated Copolymers by Copper-Mediated Living Radical Polymerization. *Macromolecules* **2003**, *36*, 9042–9049.

(42) Yurdacan, M.; Franke, O.; Hogen-Esch, T. Nanoindentation of Films of Perfluorotridecyl, Perfluorodecyl, and Perfluoroheptyl End-Functionalized Polystyrene at the Micron Scale. *Macromol. Chem. Phys.* **2016**, *217*, 1260–1269.

(43) Zhang, Y.; Park, A.; Cintora, A.; McMillan, S. R.; Harmon, N. J.; Moehle, A.; Flatté, M. E.; Fuchs, G. D.; Ober, C. K. Impact of the Synthesis Method on the Solid-State Charge Transport of Radical Polymers. *J. Mater. Chem. C* **2018**, *6*, 111–118.

(44) Guazzelli, E.; Lusiani, N.; Monni, G.; Oliva, M.; Pelosi, C.; Wurm, F. R.; Pretti, C.; Martinelli, E. Amphiphilic Polyphosphonate Copolymers as New Additives for PDMS-Based Antifouling Coatings. *Polymer* **2021**, *13*, 3414.

(45) Pretti, C.; Oliva, M.; Mennillo, E.; Barbaglia, M.; Funel, M.; Reddy Yasani, B.; Martinelli, E.; Galli, G. An Ecotoxicological Study on Tin- and Bismuth-Catalysed PDMS Based Coatings Containing a Surface-Active Polymer. *Ecotoxicol. Environ. Saf.* **2013**, *98*, 250–256.

(46) Ruben, B.; Elisa, M.; Leandro, L.; Victor, M.; Gloria, G.; Marina, S.; Mian, K. S.; Pandiyan, R.; Nadhira, L. Oxygen Plasma Treatments of Polydimethylsiloxane Surfaces: Effect of the Atomic Oxygen on Capillary Flow in the Microchannels. *Micro Nano Lett.* **2017**, *12*, 754–757.

(47) Martinelli, E.; Pretti, C.; Oliva, M.; Gisenti, A.; Galli, G. Sol-Gel Polysiloxane Films Containing Different Surface-Active Trialkoxysilanes for the Release of the Marine Fouling Ficopomatus Enigmaticus. *Polymer* **2018**, *145*, 426–433.

(48) Gevaux, L.; Lejars, M.; Margaillan, A.; Briand, J.-F.; Bunet, R.; Bressy, C. Hydrolyzable Additive-Based Silicone Elastomers: A New Approach for Antifouling Coatings. *Polymers* **2019**, *305*.

(49) Guazzelli, E.; Martinelli, E.; Pelloquet, L.; Briand, J.-F.; Margaillan, A.; Bunet, R.; Galli, G.; Bressy, C. Amphiphilic Hydrolyzable Polydimethylsiloxane-b-poly(ethylene glycol methacrylate-co-trialkylsilyl methacrylate) Block Copolymers for Marine Coatings. II. Antifouling Laboratory Tests and Field Trials. *Biofouling* **2020**, *36*, 378–388.

(50) Martinelli, E.; Gunes, D.; Wenning, B. M.; Ober, C. K.; Finlay, J. A.; Callow, M. E.; Callow, J. A.; Di Fino, A.; Clare, A. S.; Galli, G. Effects of Surface-Active Block Copolymers with Oxyethylene and Fluoroalkyl Side Chains on the Antifouling Performance of Silicone-Based Films. *Biofouling* **2016**, *32*, 81–93.

(51) Vucko, M. J.; Poole, A. J.; Carl, C.; Sexton, B. A.; Glenn, F. L.; Whalan, S.; de Nys, R. Using Textured PDMS to Prevent Settlement and Enhance Release of Marine Fouling Organisms. *Biofouling* **2014**, *30*, 1–16.

(52) Wrangle, A.-L.; Barboza, F. R.; Ferreira, J.; Eriksson-Wiklund, A.-K.; Ytreberg, E.; Jonsson, P. R.; Watermann, B.; Dahlström, M. Monitoring Biofouling as a Management Tool for Reducing Toxic Antifouling Practices in the Baltic Sea. *J. Environ. Manage.* **2020**, *264*, No. 110447.

(53) Yee, A.; Mackie, J.; Pernet, B. The Distribution and Unexpected Genetic Diversity of the Non-Indigenous Annelid *Ficopomatus enigmaticus* in California. *Aquat. Invasions* **2019**, *14*, 250–266.

(54) Okamoto, K.; Watanabe, A.; Watanabe, N.; Sakata, K. Induction of Larval Metamorphosis in Serpulid Polychaetes by L-DOPA and Catecholamines. *Fish. Sci.* **1995**, *61*, 69–74.

(55) Tilman, H.; Pei-Yuan, Q. Induction of Larval Attachment and Metamorphosis in the Serpulid Polychaete *Hydroides elegans* by Dissolved Free Amino Acids: Isolation and Identification. *Mar. Eco. Prog. Ser.* **1999**, *179*, 259–271.

(56) Matsuura, H.; Yazaki, I.; Okino, T. Induction of Larval Metamorphosis in the Sea Cucumber *Apostichopus japonicus* by Neurotransmitters. *Fish. Sci.* **2009**, *75*, 777–783.

(57) Okano, K.; Shimizu, K.; Satuito, C.; Fusetani, N. Visualization of Cement Exocytosis in the Cypris Cement Gland of the Barnacle *Megabalanus rosa*. *J. Exp. Biol.* **1996**, *199*, 2131–2137.

□ Recommended by ACS

Comparing Water Transport Properties of Janus Membranes Fabricated from Copper Mesh and Foam Using a Femtosecond Laser

Vadim Sh. Yalishev, Ali S. Alnaser, *et al.*

JANUARY 25, 2023

LANGMUIR

READ ▾

Humidity-Responsive Antimicrobial Membranes Based on Cross-Linked Copolymers Functionalized with Ionic Liquid Moieties

Denisa Druvari, Ioannis K. Kallitsis, *et al.*

FEBRUARY 14, 2023

ACS APPLIED MATERIALS & INTERFACES

READ ▾

Photo-Thermal Superhydrophobic Sponge for Highly Efficient Anti-Icing and De-Icing

Bo Yu, Feng Zhou, *et al.*

JANUARY 15, 2023

LANGMUIR

READ ▾

A Sandwich Structure of Fulvic Acid and PMIDA-Modified LDHs for the Simultaneous Removal of Cu²⁺ and Aniline in Multicomponent Solutions

Keji Wan, Zhenyong Miao, *et al.*

FEBRUARY 09, 2023

LANGMUIR

READ ▾

Get More Suggestions >